Journal of Ambient Intelligence and Humanized Computing
https://doi.org/10.1007/s12652-018-0700-z

ORIGINAL RESEARCH

Numerical modeling of electromagnetic wave logging while drilling in deviated well

Aiping Wu[1,2] · Qingqing Fu[1,2] · Saleh Muhamed Mwachaka[1,3] · Xiaoying He[1]

Received: 14 November 2017 / Accepted: 6 February 2018

Abstract
Electromagnetic wave logging-while-drilling (LWD) tools are used in geosteering for hydrocarbon exploration. Comparing with vertical wells, the response of logging has widely changed because the electrical parameters surrounding the borehole are nonaxisymmetrical distribution in deviated well. In this paper, with the method of alternating-direction-implicit finite-difference time-domain (ADI-FDTD), we discuss the logging response of electromagnetic wave LWD in deviated well, three-dimensional Yee's non-uniform staggered grid is used in cylindrical coordinates, transfer coordinate system is built between strata space and instrument space, which the conductivity tensor of the anisotropic and dipping formation can be expressed in coordinates of instrument, the method of area weighted average is used to compute the effective conductivity of partially-filled grid cells at interfaces, and uniaxial perfectly matched layer (UPML) absorbing boundary conditions is used to truncate the computational domain. Result shows that horn of logging response curve is appeared on both upper and lower boundaries, when electromagnetic wave LWD tool penetrating through the boundary with large dipping angle, and this horn is used to indicate the presence of formation boundaries. What's more, with the eccentric distance increases, horns effect of the boundary is more obvious.

Keywords Electromagnetic wave · Logging while drilling (LWD) · Finite-difference time-domain (FDTD) · Well logging

1 Introduction

In the exploration of oil and gas resources, the resistivity based on conductive characteristics of the reservoir is the basis of the qualitative evaluation whether the formation is oil-bearing strata, oil or water-bearing layer, and it is also one of the important parameters of the reservoir hydrocarbon saturation (Gorbatenko et al. 2016; Sun et al. 2016; Qin et al. 2017). LWD has the characteristics of real-time and high efficiency, which can effectively reduce the influence of drilling fluid invasion on the formation (Bakr et al. 2017; Wang et al. 2017; Shao et al. 2017), and it is significance to accurate evaluation of reservoir oil-bearing. In order to enhance oil recovery and reduce costs, horizontal wells, deviate wells and multilateral wells are used, and the number of these wells is increasing. Comparing with vertical wells, the response of logging has changed because the electrical parameters around the wellbore are no longer axially symmetric. currently, the research on electric logging of modeling and inversion numerical simulation based on horizontal wells and deviate wells is the hotspot (Yang et al. 2013). However, in the environment of logging in highly-deviated wells and horizontal wells, measure the deviation, tool eccentricity (Hong et al. 2017; Galsa et al. 2016), mud invasionand formation of the electrical anisotropy and other factors will affect the formation resistivity (Salazar et al. 2009, 2011; Zhou et al. 2015). Therefore, it is particularly important to know how to deal with the logging response characteristics of the instrument under the complicated conditions.

Meanwhile, in the processing oil drilling, it is urgent need a LWD system that can carry out real-time geosteering and it is suit to the complex oil and gas layer, predict the undrilled

✉ Qingqing Fu
jpufqq@yangtzeu.edu.cn

[1] School of Electronics and Information, Yangtze University, Jingzhou 434023, China

[2] National Demonstration Center for Experimental Electrical and Electronical Education, Yangtze University, Jingzhou, China

[3] Faculty of Computing, Information Systems and Mathematics, Institute of Finance Management, 3918 Dar es Salaam, Tanzania

Published online: 13 February 2018

formation to maintain the borehole within the desired geological. Azimuthal resistivity LWD tools with tilted antennas (Bittar 2002) are widely used in geosteering because of their azimuthal sensitivity and the relatively large depth of investigation compared with other LWD tools. Compared with conventional resistivity tools, azimuthal-resistivity LWD measurements can provide additional information including distance-to-boundary, relative dip angle, and resistivity anisotropy (Chen et al. 2016). In recent years, based on the techniques of traditional resistivity LWD, the azimuth electromagnetic wave resistivity LWD was developed and used in the oil field, but how to improve the accuracy of logging interpretation. By studying characteristics of logging response in forward modeling, the response of azimuth electromagnetic resistivity LWD in complex conditions is get, and it provides a theoretical basis for the inversion calculation and interpretation of logging data for the future.

The remainder of this paper is organized as follows. In Sect. 2 provides an overview of the numerical methods about LWD. Section 3 presents the method of ADI-FDTD for the electromagnetic wave logging while drilling. Section 4 describes the ADI-FDTD results against NMM results and presents some results for various model. Finally Sect. 5 concludes by remarking achieved results.

2 Related Works

In recent years, various numerical methods have been applied to study the response of electromagnetic wave logging in geophysical formations, such as the numerical matching method (NMM) (Fan et al. 2000), the finite element method(FEM) (Nam et al. 2013), the finite difference frequency domain(FDFD) (Hou et al. 2006), and FDTD method (Lee et al. 2012). Among these methods, those based on the direct discretization of Maxwell's equations are very flexible in handling complex media and geometries. FDTD is particularly attractive since it is easily implemented and is matrix-free, having low computational complexity that scales only linearly with the number of degrees of freedom. The FDTD method can accurately model complex LWD environments. A merit of this method is its capability of providing real-time simulation results, which are fundamental to time-domain logging tools. However,because FDTD simulation time-step sizes are limited by the smallest mesh size following the Courant stability condition, small mesh sizes lead to small time-step sizes in FDTD simulations (Wu et al. 2008), and in deviated well drilling, anisotropic formations can lead to borehole problems with dipping-layered media having full 3×3 conductivity tensors (Weiss et al. 2002).

In this context, considering on development of instrument for the future, we focuses on the key technologies of azimuth electromagnetic wave resistivity LWD, study on the forward numerical simulation of logging response with the theoretical basis of electromagnetic theory, electrical logging method and electronic information technology. In this paper, based on the principle analysis of calculation method and electromagnetic wave LWD, we employ ADI-FDTD directly with Yee's non-uniform staggered grid in three-dimensional cylindrical coordinates, transfer coordinate system between strata space and instrument space, which the conductivity tensor of the anisotropic and dipping formation can be expressed in coordinates of instrument, use area weighted average to compute the effective conductivity of partially-filled grid cells at interfaces and use UPML absorbing boundary conditions to truncate the computational domain. The proposed ADI-FDTD method is validated against NMM results in layered formations and used to simulate LWD tool response for anisotropic dipping beds in deviate well, and applied to extract the response of electromagnetic wave LWD under different combinations of eccentricity offsets.Based on the forward modeling, the logging response characteristics of electromagnetic resistivity LWD is studied, it is not only provides a theoretical basis for the logging data processing and interpretation, but also provides a guidance of design methodology for the development of instrument.

3 Method numerical formulation

3.1 FDTD method for electromagnetic field in cylindrical coordinates

Maxwell equations are a set of basic equations describing the macroscopic electromagnetic phenomena, which can be written not only in differential form, but also in integral form (Yang et al. 2010). The FDTD method is based on the differential form of Maxwell curl equation (Taflove et al. 1975; Ala et al. 2015; Redman et al. 2016), which transforms the differential operation into difference operation directly by using difference discrete. In this way, a set of time domain advancing formula is obtained, thus realizing the sampling of continuous electromagnetic field data in a certain space and for a period of time.

For the general time-varying field, the Maxwell curl equation in lossy dielectric of underground can be written as:

$$\nabla \times \mathbf{H} = \varepsilon \frac{\partial \mathbf{E}}{\partial t} + \sigma \mathbf{E} \tag{1}$$

$$\nabla \times \mathbf{E} = -\mu \frac{\partial \mathbf{H}}{\partial t} - \sigma_m \mathbf{H} \tag{2}$$

In the formula (1) and (2), where ε, μ, σ, $\boldsymbol{E}$, and $\boldsymbol{H}$ represent dielectric permittivity, permeability, conductivity,

electric field intensity and magnetic field intensity, respectively.

However, the borehole and logging tool are cylindrical, the discrete error is inevitably increased with the rectangular grid still used in the simulation of the drilled electromagnetic logging. In order to reduce the "ladder" error caused by mesh subdivision and to better match the real logging environment, the FDTD method is adopted to simulate the logging response in Cylindrical Coordinates in this paper.

According to the rotation formula of Cylindrical Coordinates:

$$\nabla \times \mathbf{A} = \left(\frac{1}{\rho}\frac{\partial A_z}{\partial \varphi} - \frac{\partial A_\varphi}{\partial z}\right)e_\rho + \left(\frac{\partial A_\rho}{\partial z} - \frac{\partial A_z}{\partial \rho}\right)e_\varphi + \left(\frac{1}{\rho}\frac{\partial(\rho A_\varphi)}{\partial \rho} - \frac{1}{\rho}\frac{\partial A_\rho}{\partial \varphi}\right)e_z, \tag{3}$$

where e_ρ, e_φ, e_z are the unit vectors.

Based on formula (3), the Maxwell curl equation in Cylindrical Coordinates can be obtained:

$$\nabla \times E = \left(\frac{1}{\rho}\frac{\partial E_z}{\partial \varphi} - \frac{\partial E_\varphi}{\partial z}\right)e_\rho + \left(\frac{\partial E_\rho}{\partial z} - \frac{\partial E_z}{\partial \rho}\right)e_\varphi + \left(\frac{1}{\rho}\frac{\partial(\rho E_\varphi)}{\partial \rho} - \frac{1}{\rho}\frac{\partial E_\rho}{\partial \varphi}\right)e_z = -\mu\frac{\partial H}{\partial t} \tag{4}$$

$$\nabla \times H = \left(\frac{1}{\rho}\frac{\partial H_z}{\partial \varphi} - \frac{\partial H_\varphi}{\partial z}\right)e_\rho + \left(\frac{\partial H_\rho}{\partial z} - \frac{\partial H_z}{\partial \rho}\right)e_\varphi + \left(\frac{1}{\rho}\frac{\partial(\rho H_\varphi)}{\partial \rho} - \frac{1}{\rho}\frac{\partial H_\rho}{\partial \varphi}\right)e_z = \varepsilon\frac{\partial E}{\partial t} + \sigma E. \tag{5}$$

Based on formula 4 ~ 5, the electric (magnetic) field values at any point on the spatial grid are related to the following three factors: (a) The electric (magnetic) field value of the point in the previous time step; (b) Magnetic (electric) field value at the last time step near on the orthogonal plane of the electric (magnetic) field; (c) Dielectric parameters σ and ε, and magnetic parameters of medium μ and σ_m. Therefore, according to a set of basic formulas of FDTD, the calculation of the electric and magnetic fields can be performed in order of points at any given time step.

3.2 Absorbing boundary condition

In the conventional FDTD, it is necessary to limit the size of spatial discrete step and time step in consideration of the requirement of calculation accuracy and stability. After determining the space step, the selection of time step needs to satisfy the Courant condition. And, in order to simulate the characteristics of electromagnetic field, the space step size must be small, which leads to the increase of the total number of time steps in the determination time and the difficulty of calculation. Therefore, the ADI-FDTD method is adopted to simulate the electromagnetic logging response of LWD (Garcia et al. 2002). This method has the characteristics of unconditional stability, that is, the selection of the time step is not limited by the space step size. When using the finite difference time domain method to calculate the electromagnetic field, it is necessary to establish the Yee's grid computing space in the whole area (Yee 1966). And, for each time step, the six field components of the electric field and magnetic field on each grid in the computational region are stored for the next time step in the calculation. Thus, the greater the calculation area, the greater the amount of storage needed. However, the calculation of FDTD must be carried out in a limited area due to any computer memory is limited. So, for the infinite grid space, the grid space is truncated somewhere in the actual calculation to conduct the equivalence of finite space and infinite space, however it will lead to the non physical electromagnetic wave reflection at the truncation of the grid space and seriously affects the accuracy of the calculation. Hence, it is necessary to take essential measures for the boundary of the truncated space, to keep the state of spreading outwards of the electromagnetic wave propagating outward at the boundary. Considering that the introduced boundary condition needs to match the ADI-FDTD difference scheme without destroying the unconditional stability principle of time step, the UPML boundary conditions and ADI-FDTD method are adopted for numerical simulation analysis in this paper.

3.3 Coordinate transformation

In the Cartesian Coordinates, the conductivity of the formation can be expressed as a diagonal tensor for a laterally homogeneous anisotropic formation, namely:

$$\overline{\sigma'} = \begin{bmatrix} \sigma_h & 0 & 0 \\ 0 & \sigma_h & 0 \\ 0 & 0 & \sigma_v \end{bmatrix}. \tag{6}$$

Here, σ_h and σ_v represent horizontal conductivity and vertical conductivity, respectively. k is anisotropic ratio,

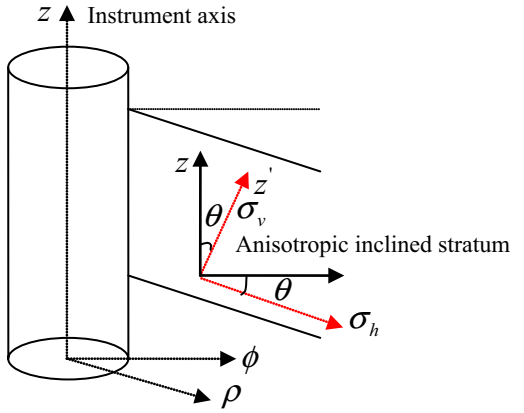

Fig. 1 Illustration of the LWD tool in formation with an anisotropic dipping bed

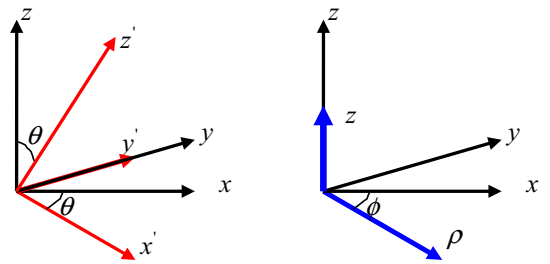

(a) First coordinate transformation **(b)** Second coordinate transformation

Fig. 2 The rotation of coordinate

$k = \left(\sigma_h/\sigma_v\right)^{1/2}$. However, in the stratum space, the principal axis of the instrument is inconsistent with the Z axis of the coordinate system, and the Cartesian coordinate system of conductivity matrix tensor of the formation does not coincide with the Cylindrical coordinate system of logging instrument, as shown in Fig. 1.

Through the two steps coordinate rotation transformation, the tensor of the conductivity matrix that expressed in the stratum space rectangular coordinate system can be expressed in the cylindrical coordinate system based on Z axis of instrument by using a rotation matrix (Lee et al. 2007). Specific methods are as follows:

First: Rotate the Cartesian coordinate system x', y', z' around the y axis with angle θ, to get rectangular coordinate system x, y, z, as shown in Fig. 2. And, θ means the angle between the direction of the principal axis of z' and z.

$$\begin{bmatrix} x' \\ y' \\ z' \end{bmatrix} = R(\theta) \begin{bmatrix} x \\ y \\ z \end{bmatrix}. \tag{7}$$

Here, $R(\theta) = \begin{bmatrix} \cos\theta & 0 & -\sin\theta \\ 0 & 1 & 0 \\ \sin\theta & 0 & \cos\theta \end{bmatrix}$.

As the Ohm's law is established in any coordinate system, and the vector field in the two coordinate systems is also in accordance with the coordinate rotation transformation relation, we can obtain:

$$\sigma = R^{-1}(\theta)\sigma' R(\theta). \tag{8}$$

Here, $R^{-1}(\theta) = \begin{bmatrix} \cos\theta & 0 & \sin\theta \\ 0 & 1 & 0 \\ -\sin\theta & 0 & \cos\theta \end{bmatrix}$.

Second: In the instrument axis space, the conductivity tensor in the angle coordinate system is converted to the cylindrical coordinate system, as shown in Fig. 2 (b). This rotation can be expressed as follows:

$$\begin{bmatrix} x \\ y \\ z \end{bmatrix} = R(\varphi) \begin{bmatrix} \rho \\ \varphi \\ z \end{bmatrix}. \tag{9}$$

Here, $R(\varphi) = \begin{bmatrix} \cos\varphi & -\sin\varphi & 0 \\ \sin\varphi & \cos\varphi & 0 \\ 0 & 0 & 1 \end{bmatrix}$.

3.4 Excitation source setting

It is necessary to consider the simulation of the excitation source when the FDTD method is used to simulate the electromagnetic wave logging problem, that is, choosing the appropriate incident wave and adding it into the FDTD iteration with a suitable method. Assume that the initial condition of each field component is 0 when the FDTD equation is used to solve the electromagnetic field value. When t > 0, the source grid point is replaced by the source field value. However, with the increase of time step, the value of the field will propagate along the grid space and act on the medium being studied, causing the scattering and absorption phenomena. In order to shorten the time of steady state establishment and reduce the shock response, the form of time domain excitation that chosen in the design is $v_s(t) = r(t)\sin(\omega t)$, $r(t)$ is a raised cosine (RC) ramp function that can be obtained as:

$$r(t) = \begin{cases} 0 & t < 0 \\ 0.5[1 - \cos(\omega t/2\alpha)] & 0 \leqslant t \leqslant \alpha T \\ 1 & t > \alpha T \end{cases}. \tag{10}$$

Here, T and α represent the period of sine function and the number of sine waves in the duration of the slope, respectively.

This special excitation function has ideal performance. For all α, the excitation source function and its first

derivative are continuous at $t = 0$; at the same time, the function integral is 0 when α is an integer multiple of 0.5, indicating that DC offset is 0 (that is, the transmitter does not contain ultra low frequency DC signal). Based on these characteristics, the time harmonic field can reach a stable state after a relatively short time.

3.5 Electromagnetic logging response signal

The electromagnetic wave generated by the electromagnetic wave resistivity LWD tool transmitting signal to the antenna is transmitted in the formation. And, the induced electromotive force is obtained at the receiving antenna. Then, by measuring the amplitude ratio and phase difference of the induced potential signal between the receiving coils of different source distances, the phase shift resistivity and the attenuation resistivity finally are obtained by the mathematical transformation method.

The formation resistivity is derived by measuring the amplitude attenuation *EATT* of the induced voltage signal and the phase difference $\Delta\phi$ of the signal on the 2 receiving coils. The benefits of measuring those two parameters are as follows: (1) the amplitude attenuation and phase difference of the measured signals are relative values, which can reduce the influence of the size of the hole and the coil; (2) in the design of the instrument, it is not necessary to increase the circuit to remove the direct coupling signal, thus simplifying the structure of the instrument. The schematic diagram of electromagnetic LWD with three coils of single-emission and double-receiving shown in Fig. 3, where T represents transmitting coil and number of windings, R_1 and R_2 represent receiving coils, the distance between transmitting coil and receiving coil are L_1 and L_2, respectively. In addition, the voltage of the receiving coils R_1 and R_2 are V_1 and V_2, respectively, amplitude attenuation *EATT* and signal phase difference $\Delta\phi$ are expressed as:

$$EATT = 20\lg\frac{|V_2|}{|V_1|}$$
$$\Delta\phi = \phi_1 - \phi_2 \tag{11}$$

Here, $|V_2|$ and $|V_1|$ represent the modulus of coil voltage V_1 and V_2, ϕ_1 and ϕ_2 are the phase angle of receiving coil voltage V_1 and V_2, respectively.

4 Results and discussion

4.1 Algorithm verification

In order to verify the correctness of the finite difference time domain method to solve the resistivity log response of LWD in the cylindrical coordinate system, a typical model is selected to calculate and compare with NMM method in this paper.

4.1.1 Model 1

Assume that the borehole is surrounded by an infinitely thick homogeneous isotropic formation, as shown in Fig. 4. The instrument uses 3-coil structure, among them, the distance between the receiving coil R_1, R_2 and transmitting coil T are 76.2 and 60.96 cm, respectively, drill collar radius is 20.32 cm, both the radius of the transmitting coil and receiving coil are 22.86 cm, and the hole diameter is 25.4 cm. In addition, the borehole filled with isotropic oil-based mud which has a conductivity of 0.0005 S/m, and the excitation frequency is 2 MHz.

Since the model is axisymmetric, it can be calculated using a two-dimensional algorithm. Thus, a uniform discrete grid is used in the longitudinal direction and the

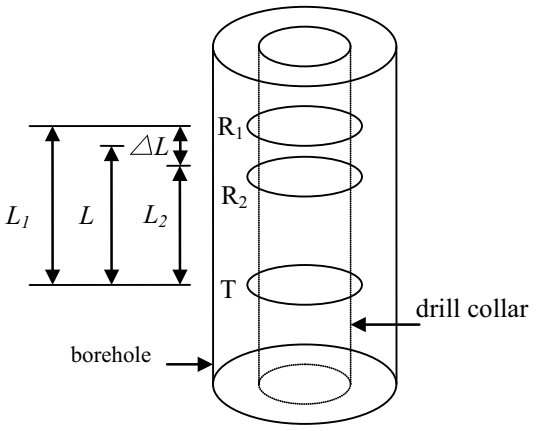

Fig. 3 Structure diagram of an electromagnetic wave resistivity LWD

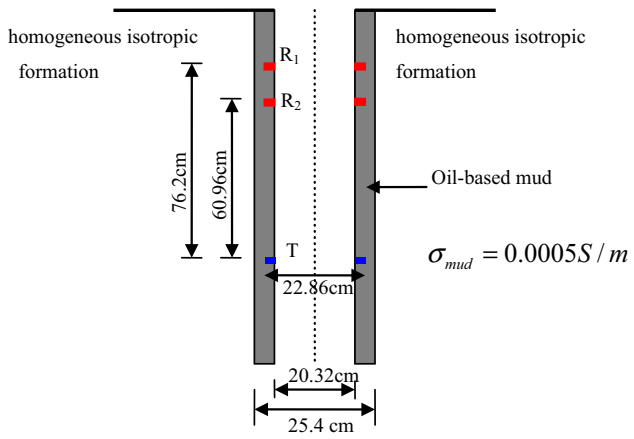

Fig. 4 Illustration of infinite thick homogeneous isotropic formation (Model1)

non-uniform grid is used in the radial direction. And, on the outside of coil, $\Delta\rho$ is gradually changed from small to large to reduce memory consumption, which value is determined by the skin depth of the maximum conductivity layer. The maximum mesh size is $(\Delta\rho)_{\max} = \delta/5$, where δ is the depth of skin corresponding to the maximum conductivity, and it is given by formula 12.

$$\delta = \frac{1}{\omega\sqrt{\mu\varepsilon}}\left\{\frac{1}{2}\left[\sqrt{1+\left(\frac{\sigma}{\omega\varepsilon}\right)^2}-1\right]\right\}^{-1/2} \tag{12}$$

When $(\sigma/(\omega\varepsilon)) \geqslant 1$, formula 12 can be simplified as:

$$\delta = \sqrt{\frac{2}{\omega\mu\sigma}}. \tag{13}$$

The calculated results of the FDTD method and the results of numerical mode matching (NMM) are shown in Fig. 5. By comparing the phase difference curve and the amplitude ratio curve, it can be seen that the results agree well with each other, which indicates that this method can be used for the simulation analysis of logging response of electromagnetic resistivity LWD.

4.2 The logging response of instrument eccentricity in isotropic formation

In the process of drilling high angle well and horizontal well, it often leads to a certain eccentricity of the instrument axis and the well shaft due to the gravity of the drilling tool and mechanical vibration during drilling. When the instrument is eccentric, it will form an asymmetrical non cylindrical electromagnetic wave, which may cause the separation of the log curve and even the formation of spikes. Therefore, it is necessary to make clear the effect of the eccentricity on the logging response to better guide the drilling and logging data.

4.2.1 Model 2

Model 2 (a) is an infinite thick homogeneous isotropic formation around the borehole, the schematic diagram of the model is shown in Fig. 6. The wellbore is filled with isotropic oil-based mud with a conductivity of 0.0005 S/m, and the surrounding strata with a conductivity of 10 S/m. Where z and z' represent instrument axis and wellbore axis, respectively. Moreover, the instrument adopts 3 coil structure. The distance between the receiving coil R_1, R_2 and transmitting coil T are76.2 and 60.96 cm, separately, drill collar radius is 20.32 cm, both the radius of the transmitting coil and receiving coil are 22.86 cm, the hole diameter is 25.4 cm, and the excitation frequency of the instrument is 2 MHz.

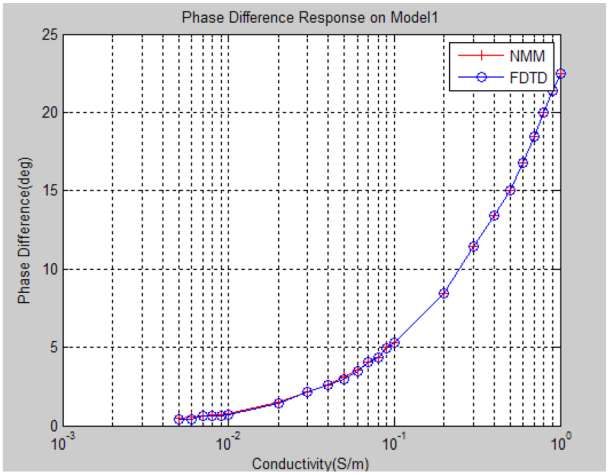

(a) Phase difference log response

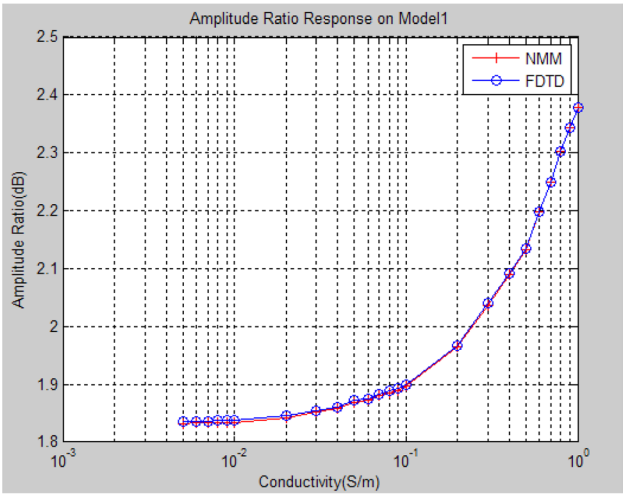

(b) Amplitude attenuation log response

Fig. 5 NMM and FDTD results for response of electromagnetic LWD tool in an infinitely homogeneous isotropic formation

In the model 2 (a), there is a great difference between the formation conductivity and the mud conductivity that the former is 20,000 times of the latter. In the direction of ρ, $\Delta\rho$ is uneven, which changes from 0.635 to 18.77 cm. And a uniform step is used in the direction of φ and z. The model 2 (b) is constructed by modifying the mud conductivity and formation conductivity of model 2 (a), in which the mud is water-based mud with a conductivity of 10 S/m, and the homogeneous formation has a conductivity of 0.1 S/m. In addition, the other model parameters are unchanged, and there is little difference between formation conductivity and mud conductivity. The partition of the grid is the same as model 2 (a), and the simulation results are shown in Fig. 7.

Figure 7 shows the simulation results of the phase difference and amplitude ratio of the instrument with the instrument offset, respectively. In the Fig. 7a, the ordinate represents the phase difference of the instrument, but

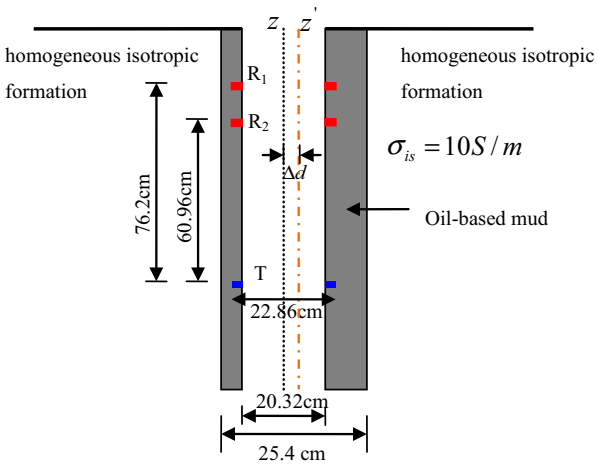

(a) Oil-based mud

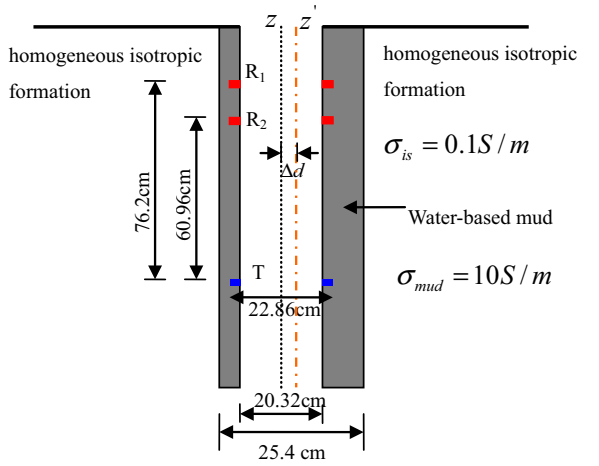

(b) Water-based mud

Fig. 6 Illustration of homogeneous isotropic infinite thick formation with eccentricity (model2)

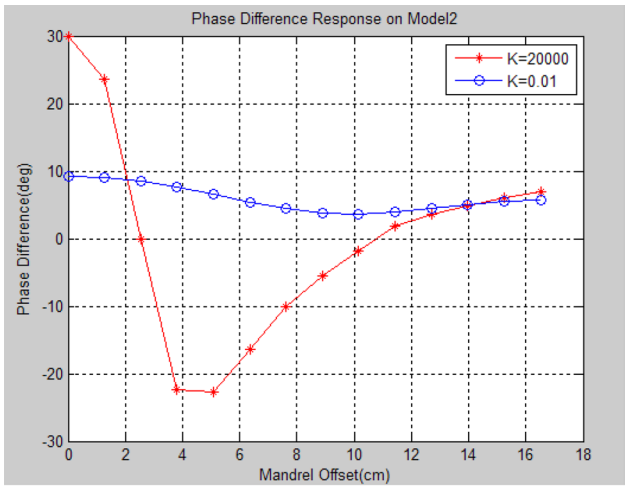

(a) Instrument eccentricity and phase difference response

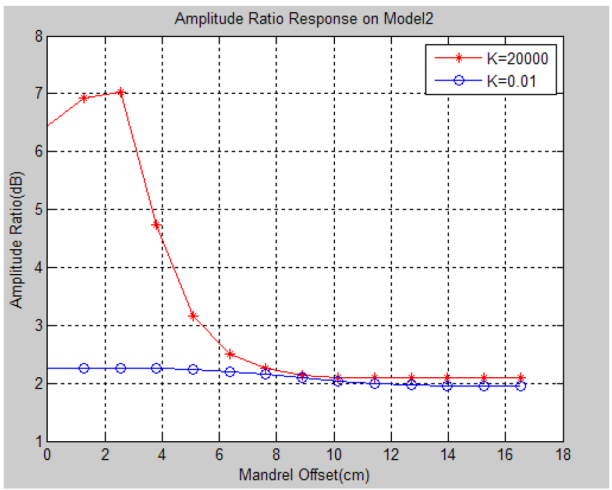

(b) Instrument eccentricity and amplitude ratio

Fig. 7 Logging response of a LWD tool with eccentricity (model2)

in Fig. 7b, the ordinate represents the amplitude ratio of the instrument, and the abscissa represents the offset of the instrument axis (the distance between the axis of the instrument and the axis of the borehole). As can be seen from the graph, when there is a great difference between mud conductivity and formation conductivity, the difference of the amplitude ratio and phase difference with the instrumental eccentricity is evident, that indicates the eccentricity of the instrument has great influence on the log response. On the contrary, when the change of conductivity (K = 0.01) is not obvious, the variation of amplitude ratio and phase difference with instrumental eccentricity is also not palpable.

The following conclusions can be obtained from the simulation of this model: in the case of large difference between mud conductivity and formation conductivity, the eccentricity of the instrument has a great influence on the log response that can not be ignored, but a little effect for the small difference.

4.2.2 Model 3

The model 3 is a three-layer formation with the upper and lower layers of an infinite uniform isotropic stratum with a conductivity of 1 S / m, and the middle is a homogeneous isotropic layer with a conductivity of 0.01 S/m. The actual thickness of the middle layer is 152.4 cm. Moreover, the isotropic oil-based mud filled in wellbore has a conductivity of 0.0005 S/m, and the instrument parameters are the same as model 2, as shown in Fig. 8.

In this model, considering the logging response of the instrument in different eccentricity and angles of the inclined isotropic formation, the discrete grid is the same as model 2. As shown in Fig. 9, the ordinate represents the amplitude

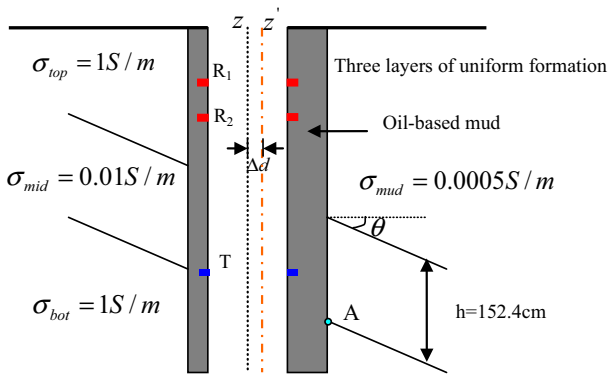

Fig. 8 Illustration of isotropic three-layer formation with eccentricity (model 3)

ratio of the instrument, and the abscissa represents the distance between the transmitter coil of the instrument and the intersection point of the lower layer with the hole, that is, the distance between the transmitter coil T and point A in Fig. 8.

It can be clearly seen from Fig. 9.

With the increase of the instrument eccentricity, the amplitude ratio changes little in the middle layer, but great in the upper layer and lower layer;

With the augment of the tilt angle, the amplitude ratio is changed at the boundary, and it has apparent change when the inclination angle is larger (greater than 60 degrees).

Through the comparative analysis, the following conclusions are drawn:

When the conductivity of the mud is different from that of the surrounding layer, the apparent resistivity varies greatly

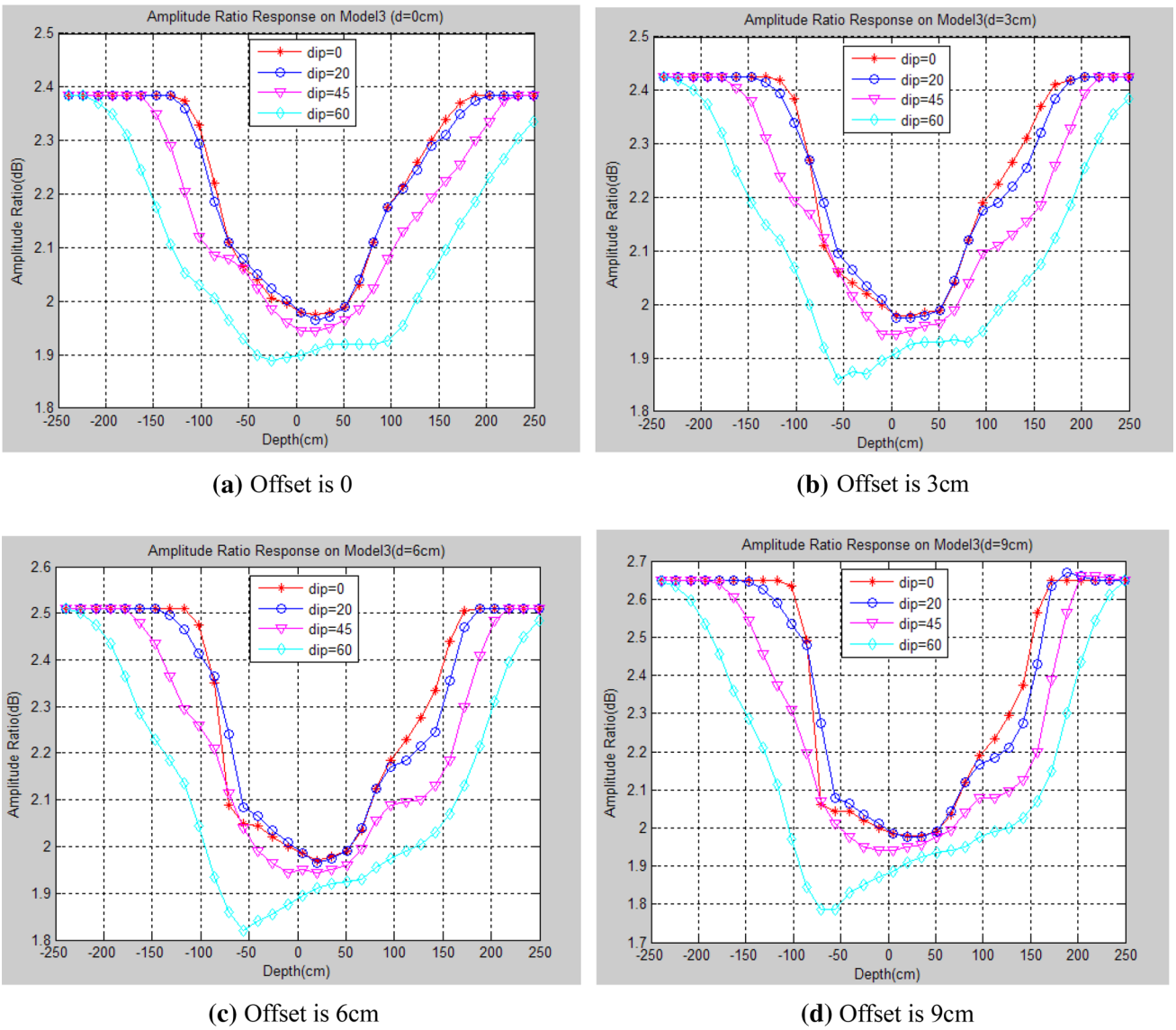

(a) Offset is 0

(b) Offset is 3cm

(c) Offset is 6cm

(d) Offset is 9cm

Fig. 9 Logging response of a LWD tool with eccentricity (model 3)

due to the eccentricity of the instrument. This is the same as in model 2.

In high angle wells, the eccentricity of the instrument increases the horn effect at the boundary.

4.3 Log response in anisotropic layered formations

4.3.1 Model 4

This model is also composed of 3 layers. Both the upper and lower layers are infinitely thick uniformly isotropic formation with a conductivity of 10 S/m, and the middle layer is a tilted anisotropic formation with a horizontal conductivity of 2.5 S/m and a vertical conductivity of 0.5 S/m. In model 4 (a), the borehole is filled with isotropic water-based mud with a conductivity of 2 S/m. And the actual thickness h of the middle layer is 152.4 cm; In model 4 (b), the borehole is filled with isotropic oil-based mud with a conductivity of 0.0005 S/m. And the actual thickness h of the middle layer also is 152.4 cm; In model 4 (c), the borehole is same as the model 4 (b), but the vertical thickness h of the middle layer is 152.4 cm. In addition, the parameters of the instrument are the same as model 2. The model is shown in Fig. 10.

In this model, the discrete grid is the same as model 2, and the log response is shown in Fig. 11. The vertical axis represents the phase difference of the instrument response, and the abscissa represents the distance between the transmitter coil T and the point A. It can be clearly seen from Fig. 11a: (1) With the increase of the dip angle, the apparent thickness of the anisotropic inclined layer becomes wider; (2) In the anisotropic formation, the phase difference decreases with the increase of the dip angle, but the influence of the dip angle on the response is not obvious in homogeneous formation; (3) At the interface of formation, the effect of horn is more obvious with the increase of dip angle.

Since the actual thickness of the strata is 152.4 cm, the vertical thickness of the anisotropic formation is also152.4 cm at $\theta = 0°$, but with the increase of the angle, the vertical layer thickness increases with sec θ factor relative to the edge of the borehole, which results in the broadening of the apparent thickness of the anisotropic tilted stratum with the increase of the dip angle; In addition, due to the increase of the electrical conductivity of the upper and lower wall rocks at the boundary of the anisotropic formation, the apparent thickness becomes wider. In vertical wells, apparent resistivity depends mainly on the horizontal conductivity, the effect of anisotropy can be ignored when the local dip is relatively small, however, the anisotropy has a great influence on the highly deviated wells and horizontal wells, and the apparent resistivity is determined by the combination of horizontal and vertical conductivity, the influence of vertical conductivity on the resistivity is also enhanced with the increase of the dip angle.

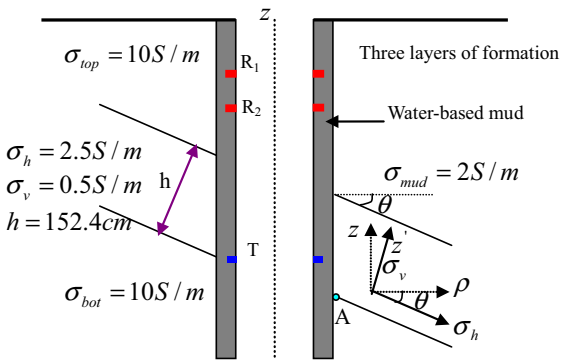

(a) Water-based mud (The actual thickness of the middle layer is 152.4cm)

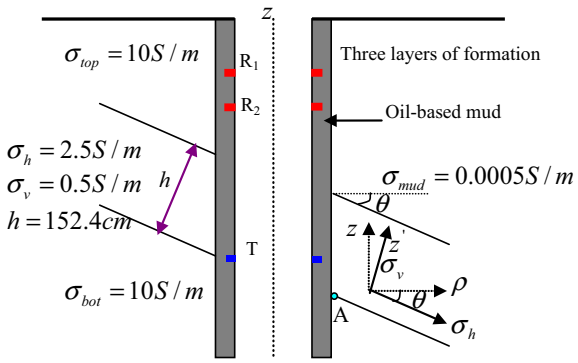

(b) Oil-based mud (The actual thickness of the middle layer is 152.4cm)

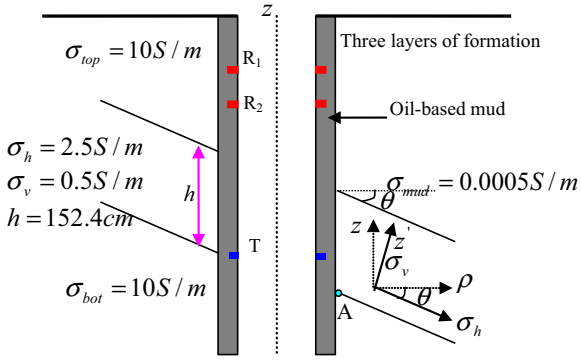

(c) Oil-based mud (The vertical thickness of the middle layer is 152.4cm)

Fig. 10 Illustration of the LWD tool in a three-layer formation with an anisotropic dipping bed

For model 4 (b), the mud is replaced with oil-based mud with a conductivity of 0.0005S/m, and the other formation parameters are the same as model 4 (a). The numerical simulation results are shown in Fig. 11b. Comparing the two diagrams of (b) and (a), it can be found that: (1) The overall responses of the instrument in the two models are very similar; (2) In the inclined stratum, the log response is sensitive to the nature of the mud. Especially that the mud conductivity increases, the apparent thickness

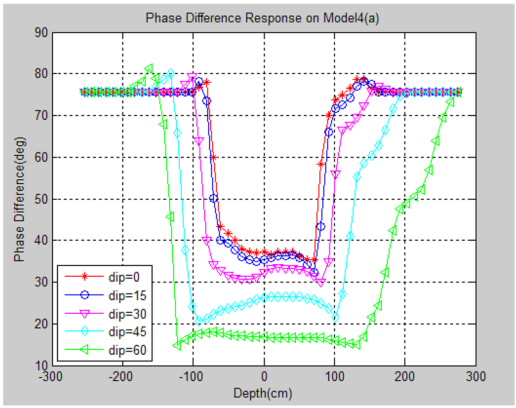

(a) Water-based mud（The actual thickness of the middle layer is 152.4cm）

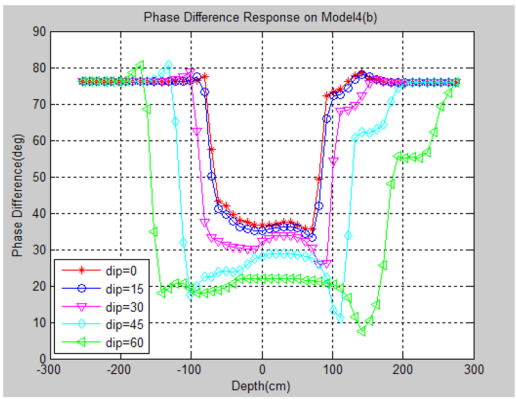

(b) Oil-based mud（The actual thickness of the middle layer is 152.4cm）

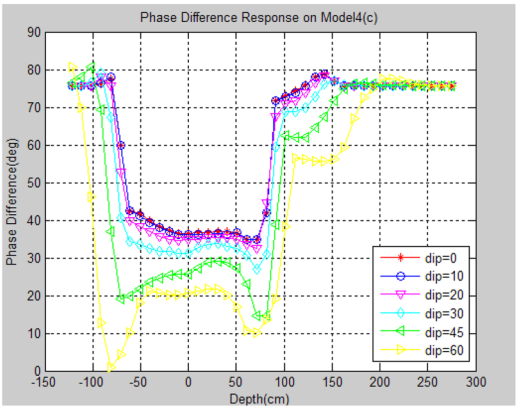

(c) Oil-based mud（The vertical thickness of the middle layer is 152.4cm）

Fig. 11 Logging response of a LWD tool with an anisotropic dipping bed (model4)

becomes wider, the phase difference becomes smaller, and the horn effect is enhanced.

For model 4 (c), oil-based mud is still selected with a conductivity of 0.0005S/m. The thickness of the anisotropic layer is fixed with respect to the axis of the instrument, and the other formation parameters are the same as those of model 4 (a). The numerical simulation results are shown in Fig. 11c. Comparing the two diagrams of (c) and (b), we can conclude: (1)The apparent thickness of model 4 (c) is reduced under large inclination angle; (2) For the large dip angle, the effect of the horn is more significant at the boundary. In the model 4 (c), the thickness of the increase in the geometric effect (sec θ) is artificially suppressed. In this case, the increase of the apparent thickness can be attributed solely to the boundary effect of the formation. Note that this is not a compression of the apparent thickness of the image (b), since the parameters of the model are constant.

Through the comparative analysis of Fig. 11, the following conclusions are drawn.

In anisotropic formation, the measurement of apparent resistivity is a comprehensive reflection of the horizontal and vertical conductivity, especially in the highly deviated-well, where the vertical conductivity has a significant effect on the response.

The dip angle of strata has an influence on log response. With the increase of the dip angle, the apparent thickness of the formation also increases; The response curve decreases with the increase of dip angle; When the tilt angle is small (less than 45°), the response curve is smooth and the inclination angle is less affected. But when the tilt angle is larger (greater than 60 degrees), the response curve has a horn effect at the boundary of the formation, and the greater the angle, the more obvious the effect of the horn.

The properties of mud have an effect on the log response. With the increase of the dip angle, the log response is sensitive to the nature of the mud, the mud conductivity increases, the apparent thickness becomes wider, the phase difference becomes smaller, and the effect of the boundary layer is enhanced.

5 Conclusion

Based on the research of the calculation methods and numerical simulation algorithms, we study the response characteristics of azimuth electromagnetic resistivity LWD in complicated conditions. In anisotropic formation, the measured apparent resistivity is a comprehensive reflection of the horizontal conductivity and vertical conductivity. The apparent thickness is widened with the inclination increases, and the horn effect can be seen in the phase difference response and amplitude ratio response for larger dipping angles, as the dipping angle is increased, the horn effect is more obvious. In general, the effect of eccentricity on the tool response is smaller when the conductivity contrast between the mud and the surrounding formation is low. Nevertheless, when the conductivity contrast between the mud and the surrounding formation is high, the effect of eccentricity on the tool response is larger, what's more, with the eccentricity increases, and the amplitude attenuation ratio is also increased. At the same dipping angle,

with the eccentric distance increases, horns effect of the boundary is more obvious. By studying characteristics of logging response in forward modeling, we are familiar with the response of electromagnetic resistivity LWD in complex conditions, it provides a theoretical basis for the inversion calculation, development of instrument independently and interpretation of logging data.

Acknowledgements The authors wish to thank the anonymous reviewers for their valuable and constructive suggestions that improved this paper. This work was partly supported by the National Natural Science Foundation of China (No. 51541408) and the Education Department of Hubei Province, China (D20141303).

References

Ala G, Francomano E, Ganci S (2015) Unconditionally stable meshless integration of time-domain maxwell's curl equations. Appl Math Comput 255(3):157–164. https://doi.org/10.1016/j.amc.2014.05.127

Bakr SA, Pardo D, Torres-Verdín C (2017) Fast inversion of logging-while-drilling resistivity measurements acquired in multiple wells. Geophysics 82(3):E111-E120. https://doi.org/10.1190/geo2016-0292.1

Bittar MS (2002). Electromagnetic wave resistivity tool having a tilted antenna for geosteering within a desired payzone. US Patent No. 6,476,609

Chen JF, Wang J, Yu Y (2016) An improved complex image theory for fast resistivity modeling and its application to geosteering. SPE J 21(4):1450–1457. https://doi.org/10.2118/170661-PA

Fan GX, Liu QH, Blanchard SP (2000) 3-d numerical mode-matching (nmm) method for resistivity well-logging tools. Antennas Propag IEEE Trans on 48(10):1544–1552. https://doi.org/10.1109/8.899671

Galsa A, Herein M, Drahos D, Herein A (2016) Effect of the eccentricity of normal resistivity borehole tools on the current field and resistivity measurement. J Appl Geophys 134:281–290. https://doi.org/10.1016/j.jappgeo.2016.09.001

Garcia SG, Lee TW, Hagness SC (2002) On the accuracy of the adi-fdtd method. Antennas Wirel Propag Lett IEEE 1(1):31–34. https://doi.org/10.1109/LAWP.2002.802583

Gorbatenko AA, Sukhorukova KV (2016) High-frequency induction logging in deviated and horizontal wells: geosteering and inversion. Russ Geol Geophys 57(7):1111–1117. https://doi.org/10.1016/j.rgg.2016.06.010

Hong D, Huang WF, Chen H, Liu QH (2017) Novel and stable formulations for the response of horizontal-coil eccentric antennas in a cylindrically multilayered medium. IEEE Trans Antennas Propag 65(4):1967–1977. https://doi.org/10.1109/TAP.2017.2670360

Hou J, Bittar MS, Hu G (2006) 3D simulation of lwd directional resistivity tool response using fdfd potential formulations. SEG Techn Progr Expand Abstr 25(1):3541. https://doi.org/10.1190/1.2370284

Lee HO, Teixeira FL (2007) Cylindrical fdtd analysis of lwd tools through anisotropic dipping-layered earth media. IEEE Trans Geosci Remote Sens 45(2):383–388. https://doi.org/10.1109/TGRS.2006.888139

Lee HO, Teixeira FL, Martin LES, Bittar MS (2012) Numerical modeling of eccentered lwd borehole sensors in dipping and fully anisotropic earth formations. IEEE Trans Geosci Remote Sens 50(3):727–735. https://doi.org/10.1109/TGRS.2011.2162736

Nam MJ, Pardo D, Torresverdín C (2013) Simulation of borehole-eccentered triaxial induction measurements using a fourierhpfinite-element method. Geophysics 78(1):D41-D52. https://doi.org/10.1190/geo2011-0524.1

Qin Z, Pan H, Wu A, Yang H, Hu T, Hou M et al. (2017). Application of conventional propagation resistivity logging for formation boundary identification in geosteering. J Geophys Eng, 14(5).https://doi.org/10.1088/1742-2140/aa80a0

Redman JD, Hans G, Diamanti N (2016) Impact of wood sample shape and size on moisture content measurement using a gpr-based sensor. IEEE J Sel Topics Appl Earth Obs Remote Sens 9(1):221–227. https://doi.org/10.1109/JSTARS.2016.2517601

Salazar JM, Torres-Verdín C (2009) Quantitative comparison of processes of oil- and water-based mud-filtrate invasion and corresponding effects on borehole resistivity measurements. Geophysics 74(1):E57. https://doi.org/10.1190/1.3033214

Salazar J, Torres-Verdin C, Wang GL (2011) Effects of surfactant-emulsified oil-based mud on borehole resistivity measurements. SPE J 16(3):608–624. https://doi.org/10.2118/109946-PA

Shao J, Yan Z, Han S, Li H, Gao T, Hu X et al (2017) Differential signal extraction for continuous wave mud pulse telemetry. J Pet Sci Eng 148:127–130. https://doi.org/10.1016/j.petrol.2016.09.047

Sun J, Gao J, Jiang Y, Cui L (2016) Resistivity and relative permittivity imaging for oil-based mud: a method and numerical simulation. J Pet Sci Eng 147:24–33. https://doi.org/10.1016/j.petrol.2016.04.042

Taflove A, Brodwin ME (1975) Numerical solution of steady-state electromagnetic scattering problems using the time-dependent maxwell's equations. IEEE Trans Microw Theory Tech 23(8):623–630. https://doi.org/10.1109/TMTT.1975.1128640

Wang H, Fehler M, Miller D (2017) Reliability of velocity measurements made by monopole acoustic logging-while-drilling tools in fast formations. Geophysics 82(4):1–30. https://doi.org/10.1190/geo2016-0387.1

Weiss CJ, Newman GA (2002) Electromagnetic induction in a fully 3-d anisotropic earth. Geophysics 67(4):1104–1114. https://doi.org/10.1190/1.1500371

Wu D, Chen J, Liu CR (2008) An efficient fdtd method for axially symmetric lwd environments. IEEE Trans Geosci Remote Sens 46(6):1652–1656. https://doi.org/10.1109/TGRS.2008.916202

Yang Y, Xiong N, Vasilakos AV, Xue J, Wang G, Zhou L (2010) A reliable quick parasitic capacitance extraction tool for the physical layer in communication systems. J Ambient Intell Humaniz Comput 1(2):75–83. https://doi.org/10.1007/s12652-009-0002-6

Yang Z, Yang J, Han L (2013) A real-time borehole correction of electromagnetic wave resistivity logging while drilling. Pet Explor Dev 40(5):671–675. https://doi.org/10.1016/S1876-3804(13)60090-7

Yee K (1966) Numerical solution of initial boundary value problems involving maxwell's equations in isotropic media. IEEE Trans Antennas Propag 14(3):302–307. https://doi.org/10.1109/TAP.1966.1138693

Zhou F, Hu XY, Meng QX, Hu XD, Liu ZY (2015) Model and method of permeability evaluation based on mud invasion effects. Appl Geophys 12(4):482–492. https://doi.org/10.1007/s11770-015-0516-y